Rapid Water Transport through Organic Layers on Ice

Xiangrui Kong, Céline Toubin, Alena Habartová, Eva Pluharova, Martina Roeselová, Jan Pettersson

THE JOURNAL OF PHYSICAL CHEMISTRY A

Article

Cite This: J. Phys. Chem. A 2018, 122, 4861−4868

pubs.acs.org/JPCA

Rapid Water Transport through Organic Layers on Ice

Xiangrui Kong,*[,†] Céline Toubin,[‡] Alena Habartova,[§] Eva Pluharova,[§,∥] Martina Roeselova,[§] and Jan B. C. Pettersson*[,†]

[†]Department of Chemistry and Molecular Biology, Atmospheric Science, University of Gothenburg, SE-41296 Gothenburg, Sweden

[‡]Laboratoire PhLAM, UMR 8523, Université de Lille, F-59000 Lille, France

[§]Institute of Organic Chemistry and Biochemistry of the Czech Academy of Sciences, Flemingovo nam. 2, CZ-16610 Prague 6, Czech Republic

[∥]J. Heyrovsky Institute of Physical Chemistry of the Czech Academy of Sciences, Dolejskova 2155/3, CZ-18223 Prague 8, Czech Republic

ABSTRACT: Processes involving atmospheric aerosol and cloud particles are affected by condensation of organic compounds that are omnipresent in the atmosphere. On ice particles, organic compounds with hydrophilic functional groups form hydrogen bonds with the ice and orient their hydrophobic groups away from the surface. The organic layer has been expected to constitute a barrier to gas uptake, but recent experimental studies suggest that the accommodation of water molecules on ice is only weakly affected by condensed short-chain alcohol layers. Here, we employ molecular dynamics simulations to study the water interactions with *n*-butanol covered ice at 200 K and show that the small effect of the condensed layer is due to efficient diffusion of water molecules along the surface plane while seeking appropriate sites to penetrate, followed by penetration driven by the combined attractive forces from butanol OH groups and water molecules within the ice. The water molecules that penetrate through the *n*-butanol layer become strongly bonded by approximately three hydrogen bonds at the butanol−ice interface. The obtained accommodation coefficient (0.81 ± 0.03) is in excellent agreement with results from previous environmental molecular beam experiments, leading to a picture where an adsorbed *n*-butanol layer does not alter the apparent accommodation coefficient but dramatically changes the detailed molecular dynamics and kinetics.

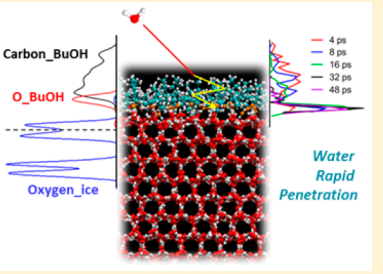

1. INTRODUCTION

Atmospheric droplets and ice particles are often coated with organic compounds,[1] which potentially change chemical reactivity[2−6] and condensation and evaporation processes[7,8] and thereby influence the properties and actions of aerosols and clouds.[9,10] Such interfacial organic layers interrupt the molecular interactions between water vapor and the water surface and may thereby influence water accommodation on ice and droplets characterized by mass accommodation coefficient (α),[11] i.e., the ratio of the number of molecules absorbed into bulk water to the number of impinging molecules. An important factor determining the barrier effect is the size and the structure of the organic molecules. Fatty acid[12,13] and long chain alcohol[14] molecules form well-ordered monolayers with their carbon tails pointing away from surface, which efficiently repel impinging gas water molecules. As surface density decreases, the long chain molecules tilt[15] and facilitate the penetration of incoming water molecules. Obviously, the permeability of a film or membrane depends on the gap between alkyl groups, which is also the reason why the presence of unsaturated fatty acids enhance the permeability of cell membranes.[16] Previous studies correlated the permeability of the organic coating with different parameters, such as integrated carbon density[17] and projected fraction coverage,[13] but such correlations are only valid for organics with similar size.

Small organics (C6 and smaller) are more prevailing in the atmosphere than larger organics, but the former ones have received less attention for their roles in influencing the mass exchange between gas and condensed phases. Among a few studies, Nathanson and co-workers used a molecular beam technique and found that a butanol monolayer on supercooled sulfuric acid solution does not impede the water transport between the gas phase and the aqueous phase.[18] On the other hand, a molecular dynamics (MD) simulation study reproduced the results for system and found that the monolayer of butanol actually reduced the accommodation coefficient by a factor of 3.[19] The discrepancy between the experimental and theoretical studies indicates that we do not fully understand the water uptake mechanism. Recently, several environmental molecular beam (EMB) studies pointed out that even though the apparent water accommodation coefficient on ice with an organic coating, e.g., *n*-butanol or *n*-hexanol, does not differ from that of clean ice, the mechanisms of the sorption and mass exchange may be significantly different.[11,20]

Gas water molecules are efficiently thermalized once they collide with a clean ice surface,[21] but before being incorporated into a strongly bonded state, the molecules are in a precursor

Received: February 26, 2018
Revised: May 5, 2018
Published: May 9, 2018

DOI: 10.1021/acs.jpca.8b01951
J. Phys. Chem. A 2018, 122, 4861−4868

state where about 1−2 hydrogen bonds are formed. These weakly bound molecules may desorb from an ice surface in milliseconds around 200 K.[21] However, when the ice is covered by an *n*-butanol film, a fraction of the impinging water molecules trap and rapidly desorb while the majority become more strongly bound and remain on the ice. These two changes counteract each other, and the apparent bulk accommodation coefficient (0.82 ± 0.09 at 190 K) is interestingly very close to that of pure ice (0.78 ± 0.09 at 190 K).[11,20] A similar effect is also seen for *n*-hexanol coated ice.[21] Even though α is similar in the different cases, it is clear that the desorption kinetics are completely altered by the existence of the organic film. Thus, unlike long-chain organics where both the condensation rate and the evaporation rate are significantly changed,[14] and therefore results in a significantly reduced accommodation coefficient, small organics allow parts of the incoming water molecules to penetrate and reach the bulk. However, due to the apparent minor effects on α, the influence of a film of short-chain organics has not received as much attention as larger organics.

To understand the role of condensed organic layers on the water uptake in greater detail, we here carry out MD simulations and look into the detailed role of *n*-butanol. The goal of this work is to provide a molecular view to complement previous EMB experiments. The MD simulations were performed in the conditions of the EMB experiments (200 K), even though this is too low to be representative of the troposphere. Particularly, in the present study we focused on the structure of the *n*-butanol monolayer, the processes of fast desorptio, and the mechanisms of water penetration through a butanol monolayer on ice.

2. METHODOLOGY

We employed classical molecular dynamics simulations with empirical force fields to investigate water accommodation on butanol-coated ice under the same conditions as previous EMB experiments.[11,20] A hexagonal ice (*Ih*) slab with the basal facets exposed to the vapor phase was prepared as described in previous studies.[22,23] Briefly, an initial ice crystal configuration of 2880 TIP5P-EW[24] water molecules at 0 K was created using the proton disordering algorithm of Buch.[25] The five-site TIP5P-EW model has been frequently used in simulation studies of ice and is capable of reproducing the experimental melting point of hexagonal ice at ambient pressure.[26] The ice sample had dimensions of about 4.4 nm, 4.6 mm, and 5.4 nm in the *x*, *y*, and *z* directions, respectively, consisting of 12 bilayers along the *z*-direction. Orientation of the *z*-axis was normal to the basal plane (0001), while the *y*-axis was perpendicular to the primary prismatic (1010) facet. The bulk ice sample was annealed over the course of a 1.5 ns *NPT* simulation at zero pressure linearly increasing the temperature from 0 to 200 K, followed by another 100 ns at 200 K to allow molecules to fully relax. Finally, the *z*-dimension of the simulation box was enlarged to 15 nm, resulting in an ice slab with two basal facet/vacuum interfaces in the *xy* plane.

The *n*-butanol was modeled by the OPLSAA force field,[27,28] and all simulations were performed using GROMACS version 4.6.3 in double precision.[29] We started with a butanol monolayer having a surface density of 4×10^{14} molecules/cm^2, i.e., 78 butanol molecules on the simulated ice surface area referring to the calculation results by Chen and co-workers.[30] For the convenience of comparing with other studies, the surface coverage is equivalent to $4 \times 10^{14} \times 4.4 \times 4.6/10^{14} = 80$ molecules in a 4.4 × 4.6 nm^2 area, which corresponds to an area per molecule equal to 26 Å^2, an area of 6.5 Å^2 per carbon atom, or a carbon density of 15 carbon atoms per nm^3. The butanol molecules were placed equidistantly (on a hexagonal grid) in the proximity of the ice surface (OH groups pointing toward the ice) and the system was equilibrated for 30 ns at 200 K, which resulted in the formation of an uniform butanol monolayer on the ice surface; i.e., neither bare ice nor partial multilayers appeared. All equilibration simulations were performed in the isochoric−isothermal *NVT* ensemble with the canonical sampling-through-velocity-rescaling thermostat with a coupling constant of 1 ps.[31] The equations of motion were integrated using the leapfrog algorithm with a time step of 1 fs. All bonds were constrained by the LINCS algorithm.[32] Three-dimensional periodic boundary conditions were applied. The short-range electrostatic and van der Waals interactions were truncated at 0.9 nm, and the long-range electrostatic interactions were treated using the particle mesh Ewald method.[33,34]

To study gas uptake processes in an analogous way as in EMB experiments,[35] one water molecule was sent toward each of the two independent interfaces from about 2.5 nm distance above (in the *z* direction) in every simulation. The initial position of the water molecule in the *xy* plane was shifted between simulations with a step of 2 Å (400 initial positions for the entire surface area), in either *x* or *y* direction, in order to randomize the collision sites. In total, 1200 trajectories are analyzed and presented in the current work. The incident beam kinetic energy (KE) was set to 0.29 ± 0.01 eV (corresponding to a velocity of 1750 ± 27 m/s; a thermal temperature of ∼2600 K) with an incident angle of 45°, which is analogous to previous EMB experimental conditions to facilitate a direct comparison.[11,21]

Unlike for the equilibration, the beam simulations were performed in the *NVE* ensemble with the time step of 1 fs, with all other parameters unchanged. 50 ps simulations were initially run to evaluate the thermalization efficiency of water molecules on the butanol-coated ice (Figure 3a). Because thermalization was concluded to be very fast, 5 ps was used in subsequent simulations (Figure 3b).

3. RESULTS AND DISCUSSION

3.1. Structure Configuration. A snapshot of the ice coated by *n*-butanol at 200 K is shown in Figure 1a, where both surfaces of the hexagonal ice slab are covered by a monolayer of *n*-butanol. Figure 1b shows the density profiles of water oxygen atoms and butanol atoms along the *z* axis. The carbon tails of butanol point away from the ice, while the oxygen atoms are preferably in contact with the uppermost water layer indicating hydrogen bond formation between the hydroxyl group of butanol and water.

The angular distribution of adsorbed butanol molecules is shown in Figure 2a, where the tilt angle (θ) is defined as the angle between a vector connecting the two extreme carbons, i.e., the carbon atom bound to the OH group and the endmost carbon on the other side of the chain, and the *z* axis that is normal to the interface (as illustrated in the inset). The sharp distributions obtained for both interfaces provide evidence for a well-organized alignment of the chains along the *z* axis, i.e. all tilted with respect to the surface normal at about 40° in order to optimize their interactions with the ice layer through the hydroxyl group and their lateral interactions, though the molecules are randomly distributed in the *x*−*y* plane.

DOI: 10.1021/acs.jpca.8b01951
J. Phys. Chem. A 2018, 122, 4861−4868

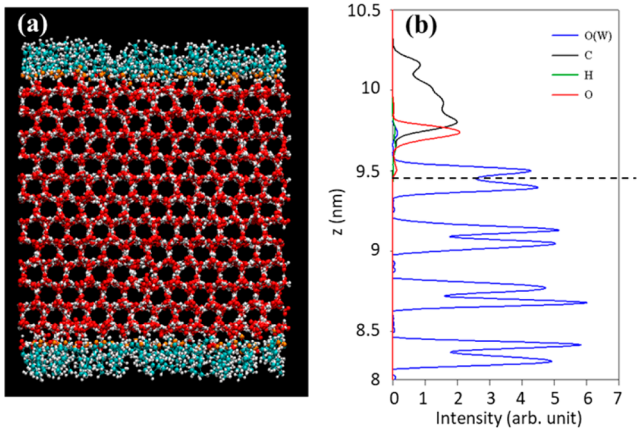

Figure 1. (a) Prismatic side view of the hexagonal ice model with a *n*-butanol monolayer at 200 K, where water oxygen is marked in red, hydrogen in white, butanol oxygen in orange, and carbon in cyan. (b) Density of water oxygen and butanol atoms along the surface normal direction, *z*, sampled over a 100 ns simulation at 200 K. The pronounced double water oxygen peaks (blue) correspond to the bilayer structure of the hexagonal ice. The dotted line marks the mid-plane of the top layer.

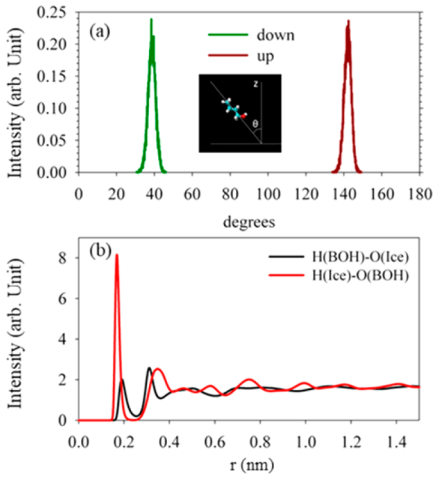

Figure 2. (a) Distribution of tilt angle characterizing the orientation of the butanol molecules on the ice surface; (b) radial distribution functions characterizing the bonding between hydrogen or oxygen atoms on butanol (BOH) and oxygen or hydrogen atoms on water (ice), respectively.

The radial distribution functions shown in Figure 2b probe the hydrogen bond formation between butanol and ice, either with butanol being "hydrogen donor" (H(BOH)−O(ice)) or with "hydrogen acceptor" (H(ice)−O(BOH)). Both distributions exhibit a pronounced peak slightly below 0.2 nm, characteristic of a hydrogen bond distance. As further support of this bonding arrangement, we calculated the average binding energies between the different compounds of the system. The average binding energy between butanol and water is slightly lower, in absolute value, than the water−water interaction, i.e., −45 kJ mol^{-1} compared to −48 kJ mol^{-1}. The magnitude of the butanol−water interaction is consistent with the formation of two hydrogen bonds as evidenced from the radial distribution function. By contrast, the lateral butanol−butanol interaction is less important, around −20 kJ/mol, attributed to van der Waals interactions between the chains. From the structural and energetic analyses we conclude that butanol molecules form well-organized layers with the C−C chains adopting similar orientations along the *z* direction mainly because of the formation of strong hydrogen bonds to water molecules. This organization implies that the hydrophilic functional group of butanol will not be directly available for incoming gas phase species. One could expect that a lower surface coverage and higher temperature may lead to a more disordered organization of the butanol monolayer at the interface, modifying significantly the accommodation of incoming water molecules.

3.2. Beam Water Impingements. Hyperthermal H_2O molecules with the velocity of 1750 ± 27 m/s were directed toward the surface at an angle of 45° from the surface normal direction, in analogy with the conditions used in EMB experiments.[11,20,21,36−38] Results of 100 trajectories are presented in Figure 3a as examples. The water molecules hit

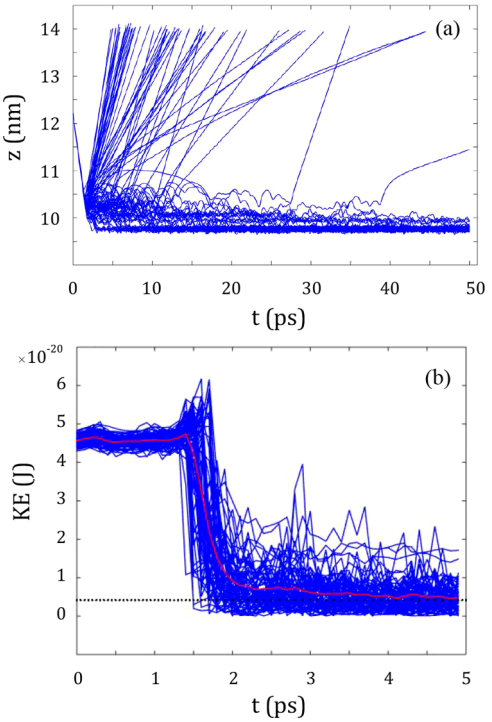

Figure 3. (a) Time evolution of the *z* coordinate of 100 impinging water molecules (rendered are oxygen atoms). (b) Kinetic energy of trapped water molecules as a function of time. The red line corresponds to the average value for 100 trajectories, and the dotted line represents the thermal kinetic energy at the surface temperature of 200 K.

the surface after 1.5−2 ps depending on the local height of the collision area. A fraction (∼20%) of the impinging water molecules are scattered within a few surface collisions and depart from the surface. Scattered molecules are often those directly hitting the outermost part of the carbon tails. In a control case (not shown) where water molecules with the same velocities impinged on neat ice with the same surface temperature, no scattering events were observed. Obviously, a butanol monolayer lowers the thermal accommodation coefficient as a result of the hydrophobicity of the alkyl chain. Within the 50 ps simulation time displayed in Figure 3a only a minority of the surface accommodated water molecules desorbs, and the majority moves deeper into the surface layer region. The quantitative accommodation coefficients based on a larger sampling size is discussed in section 3.3.

DOI: 10.1021/acs.jpca.8b01951
J. Phys. Chem. A 2018, 122, 4861−4868

Figure 3b shows the kinetic energy (KE) of thermalized amd trapped water molecules, where the red curve represents the average value for all trajectories and the black dotted line is the calculated mean thermal KE of water molecules at 200 K. The molecules initially have a constant KE until they are attracted by the surface after approximately 1.5 ps. The subsequent surface collisions result in a sharp drop in KE due to rapid energy dissipation. Within a few picoseconds all trapped water molecules release their excessive KE and become thermalized. In addition, the ice lattice underneath is also very efficient in absorbing and dispersing excessive KE from impacting molecules.[23,39]

3.3. Accommodation Coefficients. The thermal accommodation coefficient (α_t), defined as the fraction of incident water molecules completely thermalized on the surface compared to total number of impinging molecules, is calculated to be 0.81 ± 0.03 based on 1200 trajectories. Owing to the relative weak interaction between water and butanol carbon tails, rapid water desorption may take place. Thus, we defined a strict criterion to distinguish scattered and thermally desorbed molecules by examining the time that molecules spend with a KE below the thermal KE before departing from the surface. That said, the thermalized molecules include molecules that thermally desorbed within the simulation time, in addition to the ones that did not depart again. As the sampling interval time is 0.1 ps, we used the number of sampling times (n) to quantify the resident time. In an extreme case, where molecules are classified as thermalized if the residence time is 0.2 ps or longer (n = 2) before desorption, the obtained α_t is 0.84, which is an upper limit. By increase of the allowed residence time, the α_t decreases until reaching 0.78 when residence time is 1.5 ps (n = 15), and after that α_t does not decrease further with increasing residence time. Table 1 shows the dependence of α_t on the criterion determining complete thermalization.

Table 1. Thermal Accommodation Coefficients (α_t) as a Function of Time (n) That the Molecules Were Found To Have a KE Less Than the Average Thermal KE at the Surface Temperature

n	α_t
2	0.84
5	0.81
10	0.80
15	0.78
20	0.78

In an earlier simulation study, Ergin and Takahama[17] observed a correlation between integrated carbon density and water accommodation coefficient on liquid water coated with C10 and C11 alcohols. With the most compact monolayer (integrated carbon density of ∼15 carbon/nm^3), the water accommodation coefficient decreased to nearly zero. Even though this carbon density is close to the integrated carbon density of the n-butanol layer modeled in this study, a much higher accommodation coefficient is obtained here. Apparently, here the absolute length of carbon tails is the key factor of permeability. Takahama and Russell[13] compared the effective mass accommodation coefficients of ice coated by octanoic acid and myristic acid as a function of projected fractional coverages. At the same surface density (29 Å per molecule), the shorter organic monolayer made of octanoic acid shows a higher accommodation coefficient (∼0.3) than that of the longer organic myristic acid (∼0), which matches the α value for the butanol monolayer reported in this study considering the difference of carbon tails and functional groups between myristic acid and butanol.

Nathanson and co-workers performed molecular beam experiments and found that a n-butanol coating does not impede the mass transfer of either water[40] or HCl/HBr [18] out of or into a supercooled sulfuric acid solution. One reason might be that the butanol molecules are highly disordered on a liquid surface, leading to a smaller impact on mass transfer compared to that on crystalline ice surfaces. Sakaguchi et al.[19] simulated supercooled butanol coated sulfuric acid solution in a MD study and found that about 20% of the impinging water molecules are directly scattered and another 10−20% thermally desorb depending on the degree of protonation. In the same study, the authors reported the accommodation coefficient on butanol coated water, where lower accommodation coefficients of 0.58 at 213 K and 0.49 at 300 K where obtained. However, in an earlier paper from the same authors,[41] a weaker blocking effect (∼30%) of butanol on water accommodation on liquid water was observed, which is comparable to this study. Gilde et al.[42] also performed MD simulation on the effects of a butanol film on water uptake, and at a similar surface coverage as in the present study (3.6 molecules nm^{-2}) the condensation coefficient was around 42% as estimated by interpolation, which is relatively low compared to previous molecular beam[11,18,20,40] and MD simulation[19,41] studies including this work.

3.4. Fast Penetration. Trapped H_2O quickly become incorporated into the butanol-covered ice surface, as shown in a time series of the z-axis position of trapped H_2O (Figure 4). At

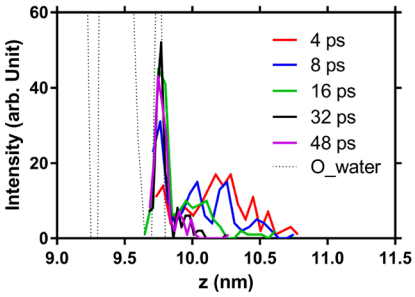

Figure 4. Time series of trapped water distribution in the z direction. The black dotted line is the density distribution of water molecules shown in Figure 1b. The result is based on analyzing 400 trajectories.

an early stage (4 ps) soon after colliding with the surface, water molecules spread in a wide range as a result of various initial impingement positions. Note that water molecules hit the butanol layer after 1.5−2 ps. At 8 ps, molecules start to accumulate next to the first water ice layer where a peak around 9.75 Å develops. As time evolves, trapped water molecules continue to move toward this region until 32 ps, after which no further changes are observed. The peak at ∼9.75 Å is at the same position as the oxygen atoms of butanol molecules, indicating that diffusing water molecules form hydrogen bonds with both ice water molecules and the OH group of butanol. Before finding a hole to penetrate, the trapped water diffuses quickly on the top of butanol layer. In average of 400 trajectories, it takes roughly 14.5 ps for half of the trapped molecules to diffuse about 5 Å on the x−y plane, which gives the median value of diffusion coefficient on the order of 10^{-9}

DOI: 10.1021/acs.jpca.8b01951
J. Phys. Chem. A 2018, 122, 4861−4868

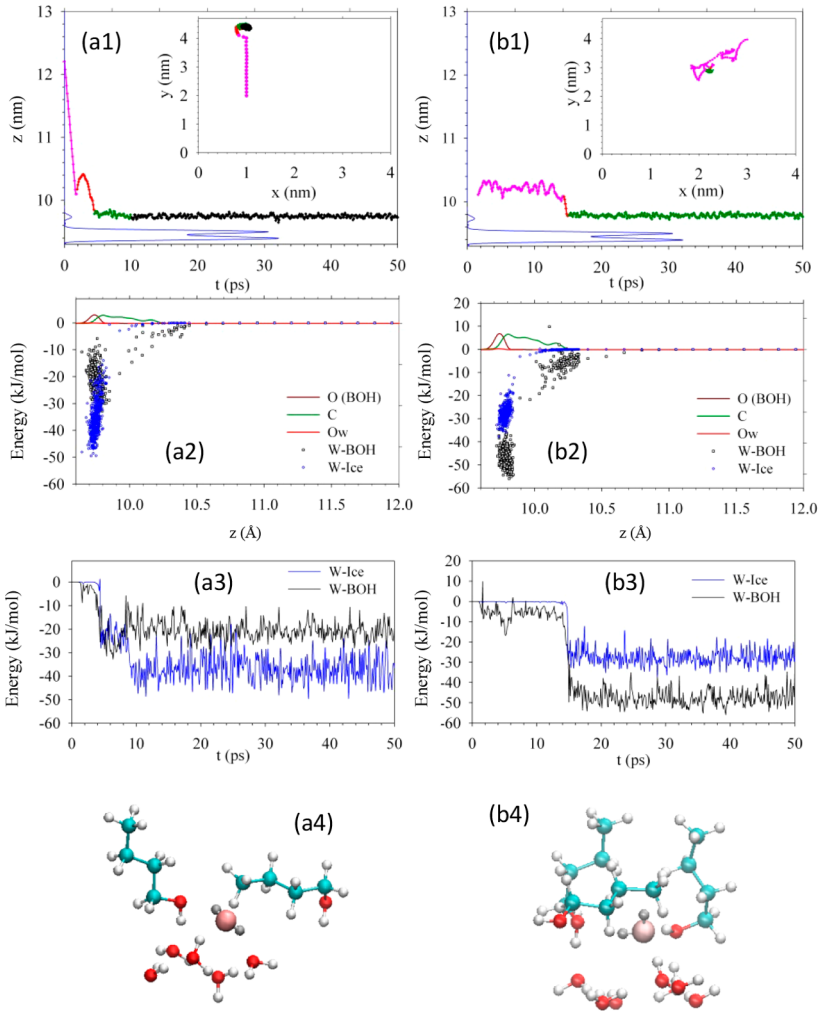

Figure 5. Example trajectories and molecular arrangements of two trapped water molecules (a, b). Top row: z coordinate of the oxygen atom of the impinging water molecule as a function of time. The water density is represented with the blue line to illustrate the location of the ice surface. The inset shows the corresponding x/y coordinates of the O of the colliding H_2O. The colors refer to the different stages that can be identified from the time-resolved z-coordinate. Second row: interaction energy between the H_2O molecule and the butanol and ice layers. Third row: time evolution of the interaction energy between the H_2O molecule and the butanol and ice layers. Bottom row: snapshot showing the first neighbors of H_2O when it is trapped between the butanol layer and the ice layer.

m^2 s^{-1}. Such value is close to the typical diffusion coefficient (D_{diff}) of water in organic liquid at room temperature.[43−44]

3.5. Individual Trajectories. In order to understand the driving force for the rapid water diffusion and the final states, two typical trajectories are analyzed in detail as shown as Figure 5a and Figure 5b. In the top panels, x-, y-, and z-coordinates of the oxygen atom of the impinging water molecule are shown as a function of time. Different stages can be identified from the time-resolved z-coordinate: the diffusion along the $x-y$ plane before finding a site to penetrate the adlayer is shown in pink, the penetration process is shown in red, and the green and black colors indicate two locations where trapped water molecules were strongly bound. The black line corresponds to a position next to the first ice layer, and green line indicates a position relatively further from the ice surface.

After reaching the surface, the incoming water molecule first rapidly diffuses on top of the butanol layer before finding a site where diffusion through the butanol layer can occur, as shown in Figure 5b1. Note that as soon as the water molecule reaches the outer range of the butanol carbon tails, the molecule is readily attracted by the OH group of butanol (Figure 5b2). This relatively weak force gently pulls water molecules toward the butanol−ice interface, but the movement is hindered by the butanol monolayer. Thus, a hole is needed for penetration. Before finding a hole to dive in, the water molecule diffuses along the hydrophobic surface, constantly pulled by the butanol OH groups. Such diffusion is mainly entropically driven and with enthalpic interference, and when a hole is available, the fast diffusion is enthalpic driven. When the incoming molecules are within a 3 Å distance from the uppermost water ice layer, an additional attractive force from water molecules in the ice applies to the mobile molecules. In combination with the hydrophobic character of the butanol chain, the trapped water molecules are effectively pulled toward the ice, as shown in Figure 5b3. Before entering the 3 Å zone, several molecules were observed to occasionally jump back and forth within the carbon tail layer, but no molecules were seen to escape from this zone. One may expect that in films consisting of longer alcohols or carboxylic acids it is difficult for water to penetrate because of three facts: (1) the landing spot will be farther away from the hydrophilic group and the attractive force that helps the "diving" movement will be weaker; (2) the ordered

DOI: 10.1021/acs.jpca.8b01951
J. Phys. Chem. A 2018, 122, 4861−4868

hydrophobic methyl groups leave less space for incoming water to penetrate; and (3) the landed molecules are farther away from the "3 Å zone". When a molecule penetrates the butanol layer and arrives at the butanol−ice interface, it forms 1−2 hydrogen bonds with ice water and simultaneously forms 1−2 hydrogen bonds with OH groups on butanol, i.e., ∼3 hydrogen bonds in total. Due to the formation of such strong bonds (Figure 5a4 and Figure 5b4), the water is locked in its position, and no further diffusion is observed on the time scale of the simulations. Moreover, this explains why the accommodation calculated in this study is comparable to that measured by EMB on a longer time scale, since it is unlikely that such strongly bound water molecules desorb on the millisecond time scale of the EMB experiments.[21]

Overall, incoming water molecules tend to move toward the ice surface due to the attractive potential from OH groups of butanol and from the ice water within a 3 Å range. The van der Waals interactions between water and the alkyl chains are much weaker than that of the hydrogen bond, which means that the presence of a butanol monolayer decreases the chance of impinging H_2O molecules to approach the strongly bound sites. The molecules that do not make it to this distance could desorb in a relative short time. However, previous EMB studies revealed that even though impinging water molecules desorb faster from a butanol coated ice surface than that from neat ice surface, on a millisecond time scale the slower desorption from neat ice surface will catch up and the bulk mass accommodation eventually become similar in the two cases.[20] On the basis of the findings from this study, we conclude that the thermal accommodation coefficient obtained here is similar to the mass accommodation coefficient from EMB experiments ($\alpha_t \approx \alpha_b$) because water molecules become bound with a higher energy on butanol-covered ice than on bare ice. Thus, the calculated accommodation coefficient from this study agrees well with the EMB results.[11,20] In a broader context, the previous experimentally obtained bulk accommodation coefficients of water on bare ice at 200 K are of smaller values than 0.81 reported here, such as 0.41 by Pettersson and co-workers,[21] 0.12−0.34 by Rossi and co-workers,[45−47] and 0.2−1.0 by Skrotzki et al.[48] Note that the thermal accommodation coefficient of water on pure ice at this temperature is unity, so the low numbers are due to the thermal desorption of adsorbed water molecules before being incorporated in the bulk. This portion is expected to be lower in the current system with a butanol coating, even in the time scales comparable to the experiments, because the impinging molecules quickly penetrate through the surfactant layer and form ∼3 hydrogen bonds to ice water and OH groups of butanol, resulting in lower evaporation rates.[49] However, evaporation is a rare event on the typical time scale of MD simulations,[50,51] so we do not directly evaluate the significance of thermal desorption in this study.

4. CONCLUSIONS

We have performed MD simulations to investigate the water accommodation on *n*-butanol coated ice at 200 K, close to the EMB experiments conditions. In the film, butanol molecules in the monolayer uniformly tilt at about 40° normal to the ice surface with the OH group pointing to the ice underneath. The radial distribution functions indicate the formation of hydrogen bonds between butanol and water ice, with a binding energy of approximately −45 kJ/mol. As gas water molecules collide with the butanol surface, some of the impinging molecules scatter after impacting the carbon tails of butanol molecules. However, the initial kinetic energy is quickly dispersed and the majority of incoming water molecules remain on the butanol layer. These molecules diffuse rapidly on the butanol surface until they find a suitable site to penetrate into the alcohol layer. Two important types of attractive forces act on the trapped water, which are the attraction from the OH-group on butanol and from the water molecules in the ice. The OH-group acts on any trapped water molecule, pulling it downward at a suitable site. As soon as the mobile water molecule is within 3 Å from the butanol−ice interface, they travel this distance quickly due to the additional attraction from ice water. Once the external water molecules penetrate the butanol layer, they become strongly bound by on average three hydrogen bonds to both butanol OH groups and ice water molecules. This explains the findings in earlier EMB experiments, where the apparent water accommodation coefficients on bare ice and butanol coated ice are similar in magnitude but rely on different kinetics.[11,21] The role of short organic films on water accommodation has been largely ignored due to their apparent minor influence, but the finding from this work illustrates how a short-chain organic coating significantly influences the dynamics of water accommodation on ice, with potential implications for their effects on ice processes and heterogeneous reactions. A forthcoming study will investigate the influence of organics coverage and water beam properties since these parameters may also impact water accommodation.

AUTHOR INFORMATION

Corresponding Authors

*X.K.: e-mail, xiangrui.kong@chem.gu.se.
*J.B.C.P.: e-mail, janp@chem.gu.se.

ORCID

Xiangrui Kong: 0000-0002-7205-0723
Jan B. C. Pettersson: 0000-0001-8420-6126

Notes

The authors declare no competing financial interest.

ACKNOWLEDGMENTS

This work is supported by the Swedish Research Council (Grant 2015-04212) and by the CaPPA project (Chemical and Physical Properties of the Atmosphere) funded by the French National Research Agency (ANR) through the PIA (Programme d'Investissement d'Avenir) under Contract ANR-11-LABX-0005-01. X.K. thanks the Swedish Research Council for an International Postdoc Fellowship (Grant 2014-6924). C.T. thanks the French Ministère de l'Enseignement Supérieur et de la Recherche, the Hauts de France Region, and the European Funds for Regional Economical Development for their financial support to this project. This work is a contribution to the CPER research project CLIMIBIO. E.P. acknowledges access to computing and storage facilities owned by parties and projects contributing to the National Grid Infrastructure. MetaCentrum provided support under the program "Projects of Large Research, Development, and Innovations Infrastructures" (CESNET LM2015042). We are very grateful to Dr. Ivan Gladich, Dr. Štěpán Timr, Dr. Nikola Marković, and Prof. Pavel Jungwirth for their valuable assistance and advice. Especially, we express the deepest honor and the memory of Martina Roeselová, with whom this work was initialized.

DOI: 10.1021/acs.jpca.8b01951
J. Phys. Chem. A 2018, 122, 4861−4868

REFERENCES

(1) Gill, P. S.; Graedel, T. E.; Weschler, C. J. Organic Films on Atmospheric Aerosol Particles, Fog Droplets, Cloud Droplets. *Rev. Geophys.* **1983**, *21*, 903−920.

(2) Shaloski, M. A.; Gord, J. R.; Staudt, S.; Quinn, S. L.; Bertram, T. H.; Nathanson, G. M. Reactions of N_2O_5 with Salty and Surfactant-Coated Glycerol: Interfacial Conversion of Br^- to Br_2 Mediated by Alkylammonium Cations. *J. Phys. Chem. A* **2017**, *121*, 3708−3719.

(3) Burden, D. K.; Johnson, A. M.; Krier, J. M.; Nathanson, G. M. The Entry of HCl through Soluble Surfactants on Sulfuric Acid: Effects of Chain Branching. *J. Phys. Chem. B* **2014**, *118*, 7993−8001.

(4) Park, S. C.; Burden, D. K.; Nathanson, G. M. Surfactant Control of Gas Transport and Reactions at the Surface of Sulfuric Acid. *Acc. Chem. Res.* **2009**, *42*, 379−387.

(5) Cosman, L. M.; Knopf, D. A.; Bertram, A. K. N_2O_5 Reactive Uptake on Aqueous Sulfuric Acid Solutions Coated with Branched and Straight-Chain Insoluble Organic Surfactants. *J. Phys. Chem. A* **2008**, *112*, 2386−2396.

(6) Thornton, J. A.; Abbatt, J. P. D. N_2O_5 Reaction on Submicron Sea Salt Aerosol: Kinetics, Products, and the Effect of Surface Active Organics. *J. Phys. Chem. A* **2005**, *109*, 10004−10012.

(7) Ma, X.; Chakraborty, P.; Henz, B. J.; Zachariah, M. R. Molecular Dynamic Simulation of Dicarboxylic Acid Coated Aqueous Aerosol: Structure and Processing of Water Vapor. *Phys. Chem. Chem. Phys.* **2011**, *13*, 9374−9384.

(8) Miles, R. E. H.; Davies, J. F.; Reid, J. P. The Influence of the Surface Composition of Mixed Monolayer Films on the Evaporation Coefficient of Water. *Phys. Chem. Chem. Phys.* **2016**, *18*, 19847−19858.

(9) Kolb, C. E.; et al. An Overview of Current Issues in the Uptake of Atmospheric Trace Gases by Aerosols and Clouds. *Atmos. Chem. Phys.* **2010**, *10*, 10561−10605.

(10) Donaldson, D. J.; Vaida, V. The Influence of Organic Films at the Air−Aqueous Boundary on Atmospheric Processes. *Chem. Rev.* **2006**, *106*, 1445−1461.

(11) Thomson, E. S.; Kong, X.; Markovic, N.; Papagiannakopoulos, P.; Pettersson, J. B. C. Collision Dynamics and Uptake of Water on Alcohol-Covered Ice. *Atmos. Chem. Phys.* **2013**, *13*, 2223−2233.

(12) Chakraborty, P.; Zachariah, M. R. Sticking Coefficient and Processing of Water Vapor on Organic-Coated Nanoaerosols. *J. Phys. Chem. A* **2008**, *112*, 966−972.

(13) Takahama, S.; Russell, L. M. A Molecular Dynamics Study of Water Mass Accommodation on Condensed Phase Water Coated by Fatty Acid Monolayers. *J. Geophys. Res.* **2011**, *116*, 14.

(14) Davies, J. F.; Miles, R. E. H.; Haddrell, A. E.; Reid, J. P. Influence of Organic Films on the Evaporation and Condensation of Water in Aerosol. *Proc. Natl. Acad. Sci. U. S. A.* **2013**, *110*, 8807−8812.

(15) Henry, D. J.; Dewan, V. I.; Prime, E. L.; Qiao, G. G.; Solomon, D. H.; Yarovsky, I. Monolayer Structure and Evaporation Resistance: A Molecular Dynamics Study of Octadecanol on Water. *J. Phys. Chem. B* **2010**, *114*, 3869−3878.

(16) Gennis, R. B. *Biomembranes: Molecular Structure and Function*; Springer, 1989.

(17) Ergin, G.; Takahama, S. Carbon Density Is an Indicator of Mass Accommodation Coefficient of Water on Organic-Coated Water Surface. *J. Phys. Chem. A* **2016**, *120*, 2885−2893.

(18) Lawrence, J. R.; Glass, S. V.; Park, S.-C.; Nathanson, G. M. Surfactant Control of Gas Uptake: Effect of Butanol Films on HCl and HBr Entry into Supercooled Sulfuric Acid. *J. Phys. Chem. A* **2005**, *109*, 7458−7465.

(19) Sakaguchi, S.; Morita, A. Molecular Dynamics Study of Water Transfer at Supercooled Sulfuric Acid Solution Surface Covered with Butanol. *J. Phys. Chem. A* **2013**, *117*, 4602−4610.

(20) Kong, X. R.; Thomson, E. S.; Papagiannakopoulos, P.; Johansson, S. M.; Pettersson, J. B. C. Water Accommodation on Ice and Organic Surfaces: Insights from Environmental Molecular Beam Experiments. *J. Phys. Chem. B* **2014**, *118*, 13378−13386.

(21) Kong, X. R.; Papagiannakopoulos, P.; Thomson, E. S.; Markovic, N.; Pettersson, J. B. C. Water Accommodation and Desorption Kinetics on Ice. *J. Phys. Chem. A* **2014**, *118*, 3973−3979.

(22) Gladich, I.; Pfalzgraff, W.; Marsalek, O.; Jungwirth, P.; Roeselova, M.; Neshyba, S. Arrhenius Analysis of Anisotropic Surface Self-Diffusion on the Prismatic Facet of Ice. *Phys. Chem. Chem. Phys.* **2011**, *13*, 19960−19969.

(23) Neshyba, S.; Nugent, E.; Roeselova, M.; Jungwirth, P. Molecular Dynamics Study of Ice-Vapor Interactions Via the Quasi-Liquid Layer. *J. Phys. Chem. C* **2009**, *113*, 4597−4604.

(24) Rick, S. W. A Reoptimization of the Five-Site Water Potential (TIP5P) for Use with Ewald Sums. *J. Chem. Phys.* **2004**, *120*, 6085−6093.

(25) Buch, V.; Sandler, P.; Sadlej, J. Simulations of H2o Solid, Liquid, and Clusters, with an Emphasis on Ferroelectric Ordering Transition in Hexagonal Ice. *J. Phys. Chem. B* **1998**, *102*, 8641−8653.

(26) Gladich, I.; Roeselova, M. Comparison of Selected Polarizable and Nonpolarizable Water Models in Molecular Dynamics Simulations of Ice I-H. *Phys. Chem. Chem. Phys.* **2012**, *14*, 11371−11385.

(27) Jorgensen, W. L.; Tirado-Rives, J. Potential Energy Functions for Atomic-Level Simulations of Water and Organic and Biomolecular Systems. *Proc. Natl. Acad. Sci. U. S. A.* **2005**, *102*, 6665−6670.

(28) Caleman, C.; van Maaren, P. J.; Hong, M. Y.; Hub, J. S.; Costa, L. T.; van der Spoel, D. Force Field Benchmark of Organic Liquids: Density, Enthalpy of Vaporization, Heat Capacities, Surface Tension, Isothermal Compressibility, Volumetric Expansion Coefficient, and Dielectric Constant. *J. Chem. Theory Comput.* **2012**, *8*, 61−74.

(29) Hess, B.; Kutzner, C.; van der Spoel, D.; Lindahl, E. Gromacs 4: Algorithms for Highly Efficient, Load-Balanced, and Scalable Molecular Simulation. *J. Chem. Theory Comput.* **2008**, *4*, 435−447.

(30) Chen, B.; Siepmann, J. I.; Klein, M. L. Vapor-Liquid Interfacial Properties of Mutually Saturated Water/1-Butanol Solutions. *J. Am. Chem. Soc.* **2002**, *124*, 12232−12237.

(31) Bussi, G.; Donadio, D.; Parrinello, M. Canonical Sampling through Velocity Rescaling. *J. Chem. Phys.* **2007**, *126*, 014101.

(32) Hess, B.; Bekker, H.; Berendsen, H. J. C.; Fraaije, J. G. E. M. Lincs: A Linear Constraint Solver for Molecular Simulations. *J. Comput. Chem.* **1997**, *18*, 1463−1472.

(33) Darden, T.; York, D.; Pedersen, L. Particle Mesh Ewald - an N.Log(N) Method for Ewald Sums in Large Systems. *J. Chem. Phys.* **1993**, *98*, 10089−10092.

(34) Essmann, U.; Perera, L.; Berkowitz, M. L.; Darden, T.; Lee, H.; Pedersen, L. G. A Smooth Particle Mesh Ewald Method. *J. Chem. Phys.* **1995**, *103*, 8577−8593.

(35) Kong, X.; Andersson, P. U.; Markovic, N.; Pettersson, J. B. C. Environmental Molecular Beam Studies of Ice Surface Processes. *Physics and Chemistry of Ice 2010*, 12th International Conference on the Physics and Chemistry of Ice (PCI-2010), Sapporo, Japan; Furukawa, Y., Sazaki, G., Uchida, T., Watanabe, N., Eds.; Hokkaido University Press: Sapporo, Japan, 2010; pp 79−88.

(36) Papagiannakopoulos, P.; Kong, X.; Thomson, E. S.; Marković, N.; Pettersson, J. B. C. Surface Transformations and Water Uptake on Liquid and Solid Butanol near the Melting Temperature. *J. Phys. Chem. C* **2013**, *117*, 6678−6685.

(37) Papagiannakopoulos, P.; Kong, X. R.; Thomson, E. S.; Pettersson, J. B. C. Water Interactions with Acetic Acid Layers on Ice and Graphite. *J. Phys. Chem. B* **2014**, *118*, 13333−13340.

(38) Thomson, E. S.; Kong, X. R.; Andersson, P. U.; Markovic, N.; Pettersson, J. B. C. Collision Dynamics and Solvation of Water Molecules in a Liquid Methanol Film. *J. Phys. Chem. Lett.* **2011**, *2*, 2174−2178.

(39) Vieceli, J.; Roeselová, M.; Potter, N.; Dang, L. X.; Garrett, B. C.; Tobias, D. J. Molecular Dynamics Simulations of Atmospheric Oxidants at the Air−Water Interface: Solvation and Accommodation of OH and O_3. *J. Phys. Chem. B* **2005**, *109*, 15876−15892.

(40) Lawrence, J. R.; Glass, S. V.; Nathanson, G. M. Evaporation of Water through Butanol Films at the Surface of Supercooled Sulfuric Acid. *J. Phys. Chem. A* **2005**, *109*, 7449−7457.

(41) Sakaguchi, S.; Morita, A. Mass Accommodation Mechanism of Water through Monolayer Films at Water/Vapor Interface. *J. Chem. Phys.* **2012**, *137*, 064701.

DOI: 10.1021/acs.jpca.8b01951
J. Phys. Chem. A 2018, 122, 4861−4868

(42) Gilde, A.; Siladke, N.; Lawrence, C. P. Molecular Dynamics Simulations of Water Transport through Butanol Films. *J. Phys. Chem. A* **2009**, *113*, 8586−8590.
(43) Lees, F. P.; Sarram, P. Diffusion Coefficient of Water in Some Organic Liquids. *J. Chem. Eng. Data* **1971**, *16*, 41−44.
(44) Easteal, A. J. Tracer Diffusion of Water in Organic Liquids. *J. Chem. Eng. Data* **1996**, *41*, 741−744.
(45) Pratte, P.; van den Bergh, H.; Rossi, M. J. The Kinetics of H_2O Vapor Condensation and Evaporation on Different Types of Ice in the Range 130−210 K. *J. Phys. Chem. A* **2006**, *110*, 3042−3058.
(46) Delval, C.; Rossi, M. J. The Kinetics of Condensation and Evaporation of H_2O from Pure Ice in the Range 173-223 K: A Quartz Crystal Microbalance Study. *Phys. Chem. Chem. Phys.* **2004**, *6*, 4665−4676.
(47) Fluckiger, B.; Rossi, M. J. Common Precursor Mechanism for the Heterogeneous Reaction of D_2O, HCl, HBr, and HOBr with Water Ice in the Range 170-230 K: Mass Accommodation Coefficients on Ice. *J. Phys. Chem. A* **2003**, *107*, 4103−4115.
(48) Skrotzki, J.; Connolly, P.; Schnaiter, M.; Saathoff, H.; Möhler, O.; Wagner, R.; Niemand, M.; Ebert, V.; Leisner, T. The Accommodation Coefficient of Water Molecules on Ice - Cirrus Cloud Studies at the Aida Simulation Chamber. *Atmos. Chem. Phys.* **2013**, *13*, 4451−4466.
(49) Kong, X. R.; Andersson, P. U.; Thomson, E. S.; Pettersson, J. B. C. Ice Formation Via Deposition Mode Nucleation on Bare and Alcohol-Covered Graphite Surfaces. *J. Phys. Chem. C* **2012**, *116*, 8964−8974.
(50) Musolino, N.; Trout, B. L. Insight into the Molecular Mechanism of Water Evaporation Via the Finite Temperature String Method. *J. Chem. Phys.* **2013**, *138*, 134707.
(51) Vieceli, J.; Roeselova, M.; Tobias, D. J. Accommodation Coefficients for Water Vapor at the Air/Water Interface. *Chem. Phys. Lett.* **2004**, *393*, 249−255.

DOI: 10.1021/acs.jpca.8b01951
J. Phys. Chem. A 2018, 122, 4861−4868